Synthesis and Physicochemical and Dynamic Mechanical Properties of a Water-Soluble Chitosan Derivative as a Biomaterial

Jaepyoung Cho,† Justin Grant,† Micheline Piquette-Miller,† and Christine Allen*,†,‡

Departments of Pharmaceutical Sciences and Chemistry, University of Toronto, 19 Russell Street, Toronto, Ontario, M5S 2S2 Canada

Received May 5, 2006; Revised Manuscript Received July 28, 2006

The physicochemical and rheological properties of a water-soluble chitosan (WSC) derivative were characterized in order to facilitate its use as a novel material for biomedical applications. The WSC was prepared by conjugating glycidyltrimethylammonium chloride (GTMAC) onto chitosan chains. Varying the molar ratio of GTMAC to chitosan from 3:1 to 6:1 produced WSCs with a degree of substitution (DS) that ranged from 56% to 74%. The WSC with the highest DS was soluble in water up to concentrations of 25 g/dL at room temperature. An increase in the polymer concentration gradually increased both the pH and conductivity of the WSC solutions. The rheological properties of the WSC solutions were found to be dependent on the salt and polymer concentrations as well as the DS value. In the absence of salt, the rheological behavior of the WSC was found to be typical of that for a polyelectrolyte in the dilute solution regime. However, the addition of salt decreased the viscosity of the polymer solution due to the reduction of electrostatic repulsions by the positively charged trimethylated ammonium groups of the WSC. In the concentrated regime, the viscosity of the WSCs was found to follow a power-law expression. The lowest DS WSC had the more favorable viscoelastic properties that were attributed to its high molecular weight, as confirmed by the stress relaxation spectra and intrinsic viscosity measurements. The effect of DS on the degree of interaction between WSC and the lipid egg phosphatidylcholine was investigated by FTIR analysis. Overall, the lower DS WSC had enhanced rheological properties and was capable of engaging in stronger intermolecular physical interactions.

Introduction

Chitosan is an abundant natural polysaccharide that is extracted from the exoskeleton of arthropods and the cell wall of fungi and may also be obtained synthetically by the deacetylation of chitin.[1,2] Chitosan is a linear copolymer of β-(1→4)-2-amido-2-deoxy-D-glucan (glucosamine) and β-(1→4)-2-acetamido-2-deoxy-D-glucan (acetylglucosamine) with well-characterized physical, mechanical, and biological properties.[3−6] The biodegradation, biocompatibility, and nontoxic properties of chitosan have also been established.[7−10] Chitosan has been tried as a biomedical material for a wide range of applications including wound healing and tissue engineering as well as gene and drug delivery.[11] Drug delivery systems including nanoparticles, micelles, gels, and films have been prepared from chitosan.[11−14] Studies have also reported that chitosan can effectively inhibit the proliferation of various tumor cells in vitro and in vivo.[15,16]

Chitosan is not soluble in media at physiological pH (i.e., pH = 7.4) but is soluble in an acidic environment (below a pH of 6.5) due to the protonation of its amine groups (pK_a = 6.5).[17] A 1% (v/v) acetic acid, lactic acid, or hydrochloric acid solution is often used to dissolve chitosan. In this way, an acidic solution is usually employed for the preparation of chitosan-based drug delivery systems. Following preparation, residual acid may remain within the drug formulation and in turn reduce the biocompatibility or nontoxicity of the delivery system as well as accelerate the degradation of some drugs.[18−21] Therefore, the presence of residual acid may limit the use of chitosan-based drug delivery systems. However, the material may be chemically modified as a means to enhance its aqueous solubility at neutral pH. For example, Sashiwa et al.[22] recently reported preparation of water-soluble chitosan (WSC) derivatives by reaction of chitosan with ethyl acrylate and further substitution of the intermediate with aliphatic diamines or aminoalkyl alcohols. Chen et al.[23] prepared water-soluble glycated chitosan derivatives by incubation of an aqueous suspension of chitosan and excess galactose followed by subsequent borohydride reduction of the intermediate Schiff bases produced. This water-soluble glycated chitosan derivative was explored as an immunoadjuvant in combination with the light-absorbing dye indocyanine green (ICG) for treatment of metastatic breast and prostate tumors.[23,24] Water-soluble *N*,*N*,*N*-trimethylated chitosan chloride was prepared by reacting methyl iodide with the amine groups of chitosan under alkaline conditions in order to obtain trimethyl derivatives with subsequent replacement of the iodide counterions with chloride ions by the addition of sodium chloride.[25] This chitosan derivative was explored for use in gene delivery and found to have an improved ability to complex DNA in comparison to unmodified chitosan.[26,27] Quaternary ammonium chitosan derivatives were also prepared and found to be completely water-soluble over a broad pH range. These quaternary ammonium chitosan derivatives were demonstrated to have antimicrobial

* Correspondence sent to Dr. C. Allen, Leslie Dan Faculty of Pharmacy, University of Toronto, 19 Russell Street, Toronto, Ontario, M5S 2S2 Canada. Phone: 416-946-8594. Fax: 416-978-8511. Email: cj.allen@utoronto.ca.

† Department of Pharmaceutical Sciences.

‡ Department of Chemistry.

10.1021/bm060436s CCC: $33.50
Published on Web 09/07/2006

activity[28−30] and were found to inhibit the proliferation of various cancer cell lines.[31,32]

In this study, we report on the synthesis and characterization of a series of water-soluble quaternary ammonium chitosan (WSC) derivatives. The chemical composition, molecular weight, ionic strength, and degree of substitution (DS) of the materials were determined using FTIR, ^{1}H NMR, pH, and conductivity measurements. The water solubility of the WSC derivatives was measured at 25 °C. The rheological properties of the derivatives as a function of the DS of the material, salt, and polymer concentrations were examined, and the results were analyzed using several rheological models. Previously, our group developed films from chitosan and egg phosphatidylcholine (ePC) for use in localized drug delivery.[19] The stability of the chitosan−ePC films was found to be largely dependent on the presence of interactions between the polymer and lipid components. Therefore, to demonstrate the potential utility of the WSC materials, with varying DS, blends of WSC and ePC were characterized by FTIR measurements. Overall, the findings from these studies establish many of the composition−property relationships of this series of WSC materials, which may in turn facilitate their tailored use in biomedical and pharmaceutical applications.

Experimental Section

Materials. Chitosan (92.5% purity) was purchased from Marinard Biotech, Inc. (QC, Canada). Glycidyltrimethylammonium chloride (GTMAC), silver nitrate ($AgNO_3$), acetone, ethanol, methanol, acetic acid (AcOH), sodium acetate (AcONa), and sodium chloride (NaCl) were reagent grade and purchased from Sigma-Aldrich Chemical Co. (ON, Canada). Egg phosphatidycholine (ePC, >99% purity) was obtained from Northern Lipids, Inc. (BC, Canada).

Characterization of Chitosan. The degree of deacetylation (DDA) of chitosan employed as the starting material for synthesis of the WSC derivatives was 92% as determined by FTIR analysis using a method described in detail elsewhere by Miya et al.[33] The FTIR spectrum of chitosan was obtained using a universal ATR spectrum-one Perkin-Elmer spectrophotometer (Perklin-Elmer, Connecticut, U.S.A.). The molecular weight of chitosan was determined by intrinsic viscosity measurements in 0.25 M acetic acid/0.25 M sodium acetate at 25 °C. The molecular weight was found to be approximately 2.2×10^5 g/mol using the Mark−Houwink−Sakurada (MHS) equation. The empirical constants for the MHS equation were $K = 1.49 \times 10^{-4}$ and $\alpha = 0.79$, as proposed by Kasaai et al.[34]

Synthesis of WSCs. The WSC was synthesized using an established method that is outlined in Scheme 1.[28] Briefly, 5 g of chitosan powder was suspended in deionized water, and then 1 mL of AcOH (i.e. ∼0.5% v/v) was added to the suspension as a catalyst.[28] The chitosan−AcOH mixture was stirred for 30 min prior to the dropwise addition of GTMAC with continuous stirring. The mole ratio of GTMAC to chitosan was varied from 3:1 to 6:1 to produce WSCs with different DS as listed in Table 1. The reaction mixture was stirred at 100 rpm at 50−60 °C for an 18-h period. Following the reaction, the undissolved polymer was removed by centrifugation of the mixture at 4000 rpm for 20 min at room temperature (Centrifuge 5804T, Eppendorf, Germany). For purification, the solution was filtered, methanol was added to remove the excess GTMAC, and the WSC was precipitated in acetone. The purification process was repeated three times, and the purified WSC was dried in a vacuum oven at 25 °C for 5 days with subsequent grinding of the product to obtain a fine powder.

Characterization of WSCs. FTIR measurements were performed to analyze the chemical composition of the WSCs synthesized at room temperature. The FTIR spectra of the WSCs were obtained using a universal ATR spectrum-one Perkin-Elmer spectrophotometer (Perklin-Elmer, Connecticut, U.S.A.). All spectra were an average of 64 scans at a resolution of 4 cm^{-1} and were repeated in triplicate. A background spectrum containing no sample was subtracted from all spectra. In addition, to confirm the successful conjugation of GTMAC to chitosan, ^{1}H NMR spectra were obtained on a Mercury 400 spectrometer (400 MHz for ^{1}H) in D_2O containing a small amount of CD_3COOD at 25 °C. The DS of the WSCs was calculated using an established titration method and eq 1 provided below.[35] Briefly, 0.1 g of WSC was dissolved in 100 mL deionized water (0.1 g/dL), and the conductivity of the WSC solution was measured as a function of the volume of 0.017 M silver nitrate ($AgNO_3$) added using a digital conductivity meter (Control Co., TX). The volume of 0.017 M $AgNO_3$, $V^*_{AgNO_3}$, that resulted in the lowest conductivity for the WSC solution was employed to calculate the DS using the following equation:

$$\mathrm{DS}(\%) = \frac{1.7 \times 10^{-5} V^*_{\mathrm{AgNO_3}}}{\left(\dfrac{W_w(\mathrm{g}) - (1.7 \times 10^{-5} V^*_{\mathrm{AgNO_3}} \times m_{\mathrm{GTMAC}})}{(m_G \times \mathrm{DDA}) + m_{\mathrm{AG}}(1 - \mathrm{DDA})}\right) \times \mathrm{DDA}} \times 100 \quad (1)$$

The numerator term is equivalent to the total number of moles of GTMAC conjugated to chitosan within 0.1 g of the WSC. The term in the denominator takes into account the average number of moles of deacetylated residues within the sample that were available for conjugation. Specifically, W_w is the weight of WSC in 100 mL (i.e., 0.100 g); m_{GTMAC} is the molecular weight of GTMAC (i.e., 151 g/mol); m_G is the molecular weight of glucosamine (i.e., 161 g/mol); and m_{AG} is the molecular weight of acetylated glucosamine (i.e., 203 g/mol). 1.7×10^{-5} corresponds to the number of moles of $AgNO_3$ in 1 mL of solution.

Measurement of Water Solubility of WSCs. Series of WSC solutions were prepared by the addition of WSC to water such that the concentration ranged from 0.2 to 20 g/dL. The transmittance of each solution was measured at 600 nm using a UV−visible spectrophotometer (Helios Gamma, Thermo Spectronic, U.K.). According to Park et al.,[36] the WSC is considered insoluble when the transmittance of the polymer solution is less than 50% of the transmittance for deionized water.

Preparation of WSC Solutions for Physicochemical and Rheological Measurements. Stock solutions of WSC (15 g/dL) were first prepared by dissolving the polymer in aqueous solutions that ranged from 0 to 0.1 M in terms of concentration of NaCl. The solutions were stirred (Corning, U.S.A.) at 100 rpm for 3 h at room temperature. The stock solutions were then further diluted to prepare a series of solutions that varied in terms of concentration of polymer, from 0.02 to 15 g/dL, by the addition of NaCl buffer. All WSC solutions were degassed for 3 h at room temperature and then stored at 4 °C overnight.

Physicochemical Characterization of WSC Solutions. pH and conductivity measurements were used to characterize the physicochemical properties of the WSC solutions as a function of salt (0−0.1 M) and polymer (0.02−15 g/dL) concentrations. The pH for each WSC solution was recorded at room temperature after being stabilized for 10 to 20 min. The conductivity (Control Co., TX) was determined for each WSC aqueous solution at 25 °C. Additionally, the conductivity was theoretically determined using the following equation:[37]

$$\text{Conductivity (S/cm)} = \sum_i N_i \lambda_i \quad (2)$$

where N_i is the equivalent concentration (mol/cm^3) and λ_i is the equivalent conductance of the ith ion (S·cm^2/mo1). λ_i is dependent on the concentration of each electrolyte added. Thus, the effect of the concentration of ions (c_i) on λ_i can be accounted for by using the Debye−Hükel−Onsager equation for a symmetrical (i.e., containing

Scheme 1. Reaction Scheme for the Conjugation of GTMAC to the Chitosan Backbone.

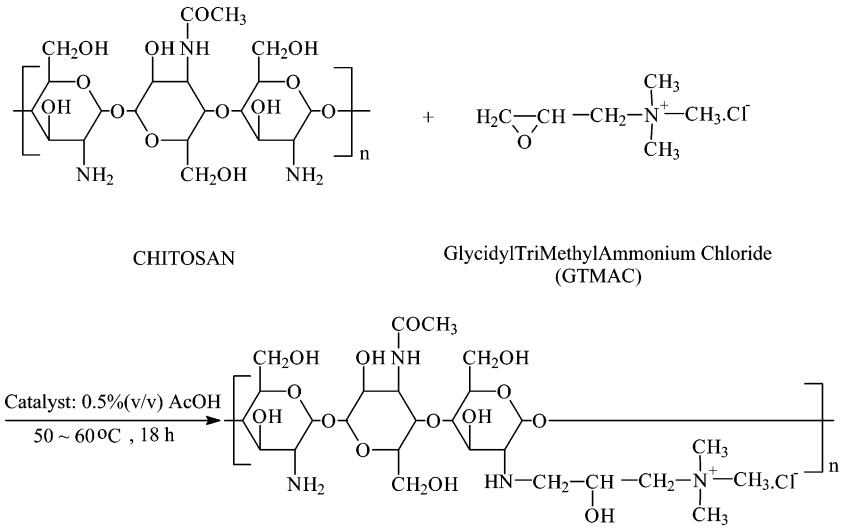

Table 1. Composition of Reaction Mixtures Employed for Preparation of WSCs with DS of 56% (G:C = 3:1), 67% (G:C 4:1), and 74% (G:C = 6:1)

chemical	G:C = 3:1	G:C = 4:1	G:C = 6:1
chitosan (C)	5 g	5 g	5 g
AcOH	1 mL	1 mL	1 mL
GTMAC (G)	13.8 mL	18.4 mL	27.6 mL
water	200 mL	195.4 mL	190.8 mL
V_{total}	214.8 mL	214.8 mL	214.8 mL

Table 2. Values for the Equivalent Conductance of Ions in the Infinite Dilute State (λ^0) at 25 °C as Obtained from Coury[39] for the Calculation of λ_i in the Debye−Hükel−Onsager Equation (eq 3)

cation	λ^o_+ (S·cm²/mol)	anion	λ^o_- (S·cm²/mol)
H^+	349.6	OH^-	199.1
Na^+	50.1	Cl^-	76.35
$(CH_3)_4N^+$	44.9		

cations and anions of equal charge) electrolyte as follows:[38]

$$\lambda_i = \lambda_i^0 - (A' + B'\lambda_i^0)c_i^{1/2} \tag{3}$$

where the constants A' and B' are 60.2 and 0.229, respectively, for a solution containing both cations and anions of unit charge at 25 °C. λ_i^0 is the equivalent conductance at infinite dilution, and the λ_i^0 value for each ion in the WSC solutions is listed in Table 2.[39] The concentrations of H^+ and OH^- ions were determined from the pH values measured for the WSC aqueous solutions. Since λ_i^0 was unknown for the positively charged trimethylated ammonium ions (WSC−$(CH_3)_3N^+$), the value of a structurally similar ammonium ion (i.e., the tetramethylammonium ion $(CH_3)_4N^+$, 44.9 S·cm²/mol) was used to approximate the conductivity of the WSC aqueous solutions.

Measurement of Rheological Properties of WSC Solutions. The viscosities of the WSC solutions were measured as a function of polymer concentration (0.02 to 15 g/dL) and in the presence of salt (0 to 0.1 M) at 25 °C. An Ostwald viscometer was used to measure the viscosity of the dilute WSC solutions with polymer concentrations below 0.5 g/dL. When the concentration was greater than 0.5 g/dL, the viscoelastic properties of the WSC solutions were characterized by a stress-controlled rheometer with a cone and plate geometry (AR-2000, TA instruments, DE). Small-amplitude oscillatory shear tests were performed in the linear viscoelastic zones (LVZ), where the complex moduli G' and G'' are independent of the magnitude of strain applied. The complex viscosity ($\eta^*(\omega)$) may be calculated using the following equation:[40]

$$\eta^*(\omega) = \frac{\sqrt{G'(\omega) + G(\omega)}}{\omega} \tag{4}$$

where $G'(\omega)$ is the storage modulus, $G''(\omega)$ is the loss modulus, and ω is the frequency applied. Assuming that the Cox−Merz rule ($\eta(\dot\gamma)|_{\dot\gamma=\omega} = |\eta^*(\omega)|$)[41] applies for the WSC solutions, the zero shear viscosity may be determined by the three-parameter Carreau model[42]

$$\eta = \frac{\eta_0}{[1 + (t_1\dot\gamma)^2]^{1-n/2}} \tag{5}$$

where t_1 is the longest relaxation time, ($\dot\gamma$) is the steady shear rate, and n is a dimensionless power index that characterizes the shear-thinning behavior of polymeric systems. The viscosities measured were used to calculate the reduced viscosity (η_{red}) in the concentrated regime as follows:[43]

$$\eta_{red} = \frac{\eta_{SP}}{C} = \frac{\eta_{P,0} - \eta_S}{\eta_S C} \tag{6}$$

where $\eta_{P,0}$ is the zero shear viscosity of each solution, η_S is the viscosity of the solvent, and C is the polymer concentration. However, in the dilute regime, the viscosities of the solutions were too low to be measured using the rheometer. Thus, the viscosity term (η) was replaced by flow time (t) to calculate η_{red} as shown in the following equation:[40]

$$\eta_{red} = \frac{\eta_{SP}}{C} = \frac{t_P - t_S}{t_S C} \tag{7}$$

where t_P and t_S represent the flow times of the polymer solutions and solvent, respectively. In addition, the data obtained for the complex moduli G' and G'' data were analyzed with several different rheological models in order to understand the molecular behavior of the WSCs under the various solution conditions.

Preparation and Characterization of WSC−ePC Films. WSC-ePC films were prepared according to a method described previously in the literature, without the use of acetic acid.[19] Briefly, 200 mg of pure ePC was dissolved in ethanol and added to a 2% solution of WSC (3:1, 4:1, or 6:1 (mol/mol) GTMAC/chitosan). The WSC−ePC mixture was stirred, placed in a Teflon-coated dish and left to dry at room temperature. The interactions between WSC and ePC were analyzed by FTIR analysis as described above.

Results and Discussion

Synthesis and Characterization of WSC. The WSC derivatives were synthesized using a method previously described by

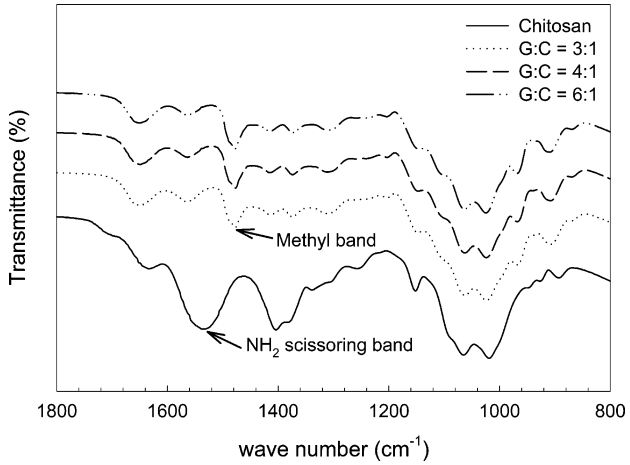

Figure 1. FTIR spectra of water-soluble chitosans (WSCs) with varying degrees of substitution (DS).

Seong et al.[28] Briefly, the derivatives were obtained by reacting chitosan with GTMAC as shown in Scheme 1. Synthesis of the quaternary ammonium chitosan derivative required the addition of a small quantity of acetic acid in order to increase the rate of reaction and to ensure the targeted conjugation of the epoxy group of GTMAC to the amine group of chitosan. Studies have shown that this epoxy group may be opened more easily in an acidic environment, which in turn results in an increase in the reaction rate.[28] Also, in an acidic environment, the epoxy group of GTMAC mostly reacts with the amine groups ($-NH_2$) of chitosan, whereas under alkaline conditions, conjugation predominantly occurs to the hydroxyl groups ($-OH$) on the chitosan backbone.[2] The DS of WSC can vary depending on the reaction conditions such as temperature, reaction time, and concentration of polymer.[28,35] In the present study, the DS of WSC was controlled by varying the molar ratio of GTMAC to chitosan (i.e., from 3:1 to 6:1 GTMAC/chitosan).

The FTIR spectra for chitosan and the synthesized WSCs are included in Figure 1. The peak corresponding to the methyl band of GTMAC at 1475 cm^{-1} was present in the spectra for all WSCs but not in the spectrum for the unmodified chitosan. Also, the band at 1550 cm^{-1} that corresponds to the primary amine group on chitosan was shifted to ~1563 cm^{-1}, and the peak areas were decreased in all spectra obtained for the WSCs. In this way, the FTIR analysis confirmed the successful conjugation of GTMAC to the amine group of chitosan.

To further confirm the success of the reaction, ^1H NMR analysis of chitosan and 56% DS WSC was performed in CD_3COOD-D_2O solution. The peak positions of each functional group in chitosan and WSC are shown in Figure 2. From the obtained NMR spectra, peaks at $\delta = \sim 1.9$ ppm ($-COCH_3$ from chitin) and $\delta = \sim 3.5 - 4.0$ ppm (C-3,4,5,6) were observed for both chitosan and WSC. However, peaks at 3.1 and 3.3 ppm were only found for WSC, which represents the $-^+N(CH_3)_3$ and $-N-CH_2-$ (labeled as c in Figure 2) groups in GTMAC, respectively. In addition, the C-2 peak at 3.1 ppm shifted to 2.9 ppm following the chemical reaction. These distinct differences between the NMR spectra for both materials further confirm the synthesis of WSC.

The DS for each WSC was quantified using a titration method that depends on conductivity measurements in the presence of varying amounts of 0.017 M $AgNO_3$ (Figure 3a).[28] Prior to the addition of $AgNO_3$, the initial conductivity was highest for the WSC prepared using a 6:1 mole ratio of GTMAC to chitosan. As $AgNO_3$ was added to the solutions of WSC, the conductivity gradually decreased. The reduction in conductivity may be explained by the following chemical reaction:

$$\text{WSC-}(CH_3)_3N^+Cl^-\,(aq) + Ag^+NO_3^-\,(aq) \leftrightarrow \text{WSC}-(CH_3)_3N^+NO_3^-\,(aq) + AgCl \quad (8)$$

The dissociation of the chloride salt of the WSC produces the positively charged trimethylated ammonium derivative and Cl^- ions, while the $AgNO_3$ solution includes Ag^+ and NO_3^- ions. The Cl^- and Ag^+ ions combine to form an insoluble solid that precipitates and in turn results in a reduction in the conductivity of the solution. The addition of the aqueous $AgNO_3$ solution to the WSC only decreases the conductivity until a minimum value is reached. A further addition of the $AgNO_3$ resulted in an increase in the conductivity of the solution. The DS values for each of the WSCs were calculated from eq 1 using the critical volume ($V^*_{AgNO_3}$) which is defined as the volume of $AgNO_3$ required to reach the minimum conductivity value (Figure 3a). As shown in Figure 3b, the calculated percentage of DS increased with an increase in the ratio of GTMAC to chitosan initially employed for synthesis (i.e., DS = 56% for 3:1, 67% for 4:1, and 74% for 6:1 GTMAC/chitosan (mol/mol)).

Water Solubility of WSCs. To determine the water solubility of the WSCs having DS of 56% or 74%, the transmittance of the polymer solutions was measured by UV−visible spectroscopy as a function of the polymer concentration. As shown in Figure 4, the transmittance was greatly dependent on the polymer concentration. When the polymer concentration was less than 1 g/dL, the transmittance was constant regardless of the DS. However, increasing the polymer concentration above 1 g/dL abruptly decreased the transmittance of both 56% and 74% DS WSC solutions. Above polymer concentrations of 6 g/dL and 12 g/dL for the WSCs with DS of 56% and 74%, respectively, the transmittance could not be measured owing to the high viscosity of the solutions. For this reason, the experimental results were fitted using a polynomial equation (solid line in Figure 4), and the curves were extrapolated to 50% transmittance in order to estimate the solubility of the WSCs in water. In this way, the water solubilities of the 56% and 74% DS WSCs were estimated to be approximately 15 g/dL and 25 g/dL, respectively. Solutions were prepared at polymer concentrations above the estimated solubility in order to evaluate the accuracy of the estimated values. Indeed, the 56% and 74% DS WSCs were found to be only partially soluble at concentrations of 20 g/dL and 30 g/dL, respectively. Therefore, the conjugation of GTMAC to the chitosan backbone provided a significant increase in the water solubility of the material.

Physicochemical Characterization of WSC Solutions. As shown in Table 3, the pH values for the WSC solutions decreased with increasing percent DS of the material. However, the pH values for the WSC solutions were found to increase as the concentration of polymer and NaCl increased. Thus, the unreacted amine groups ($-NH_2$) in the backbone of the WSCs may be partially ionized in solution. The chemical reaction for the ionization of the amine groups in chitosan may be expressed as follows:[2]

$$R-NH_3^+ + H_2O \leftrightarrow R-NH_2 + H_3O^+ \quad (9)$$

The dissociation constant (K_a) of a conjugate acid may be

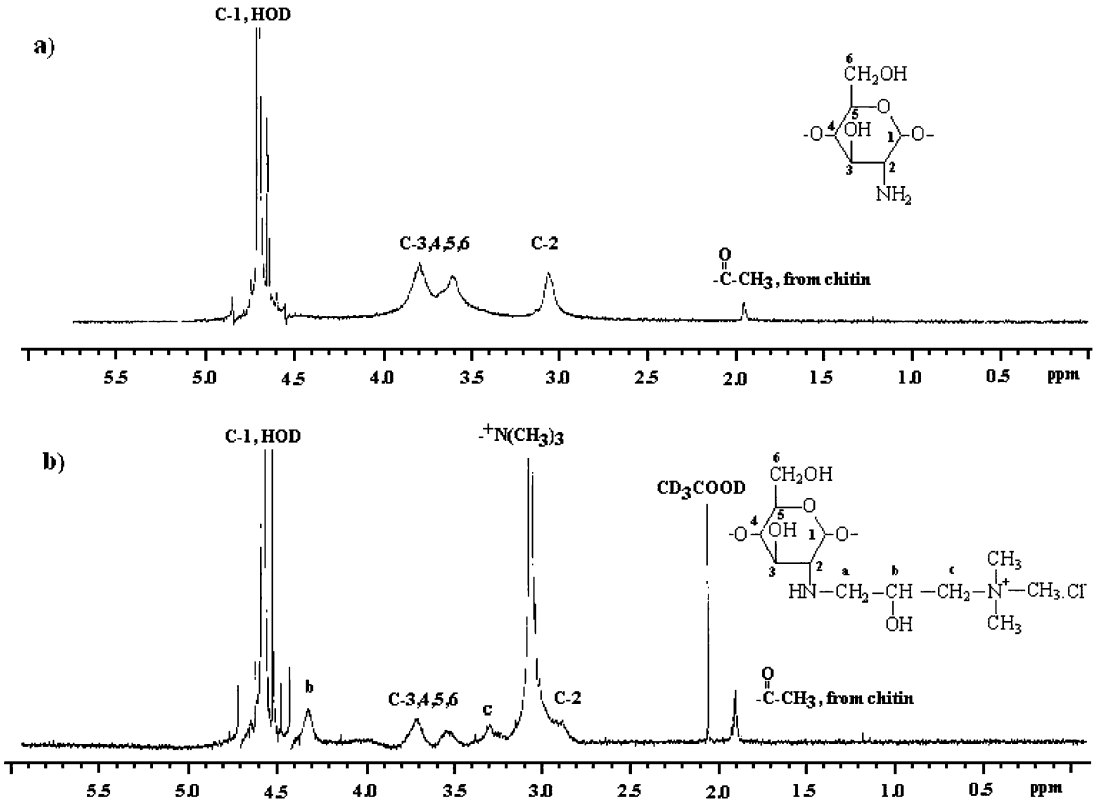

Figure 2. ^{1}H NMR spectra for (a) chitosan and (b) WSC.

defined by the following equation:[2]

$$K_a = \frac{[R-NH_2][H_3O^+]}{[R-NH_3^+]} \quad pK_a = -\log K_a \tag{10}$$

Equation 10 can be rearranged in the form of the Henderson−Hasselbalch equation[44]

$$pH = pK_a + \log\frac{[-NH_2]}{[R-NH_3^+]} \tag{11}$$

Equation 11 is only valid under ideal conditions (i.e., the ionic strength of the solution is zero). Under nonideal conditions, the dissociation constant for chitosan may be determined as follows:

$$K_a = \frac{a_{R-NH_2}a_{H_3O^+}}{a_{R-NH_3^+}} \tag{12}$$

where a is the activity of each ion and can be written in terms of units of molality (and activity coefficients γ of the solute species (i.e., $a_{R-NH_3^+} = \gamma_{R-NH_3^+}[R-NH_3^+]$). Thus, eq 11 can be modified by combining with eq 12 as follows:

$$pH = pK_a + \log\frac{[R-NH_2]}{[R-NH_3^+]} - \log\gamma_{R-NH_3^+} \tag{13}$$

At a constant temperature, the activity coefficient of an ion (γ_i) can be calculated using the Debye−Hückel equation as follows:[45]

$$\log\gamma_i = \frac{-A_m Z_i^2\sqrt{I_S}}{1 + BR_0\sqrt{I_S}} \tag{14}$$

where A_m and B are 1.17 mol$^{-1/2}$ L$^{1/2}$ and 0.329 Å^{-1} mol$^{-1/2}$ L$^{1/2}$ at 298.15 K, respectively. The ionic radius (R_0) is a fitting parameter and is between 3 and 10 Å. The combination of eqs 13 and 14 clearly shows the effect of the ionization of chitosan on the pH value of the solution as follows:

$$pH = pK_a + \log\frac{[-NH_2]}{[R-NH_3^+]} + \frac{A_m Z_{R-H_3^+}^2\sqrt{I_S}}{1 + BR_0\sqrt{I_S}} \tag{15}$$

Thus, the pH increases due to the consumption of H^+ ions during the ionization of chitosan's amine groups and the increase in ionic strength (I_S) of the solvent. From our results, the higher pH values observed for the WSC with the lower DS may be explained by the higher number of free NH_2 groups on the polymer backbone (i.e., the H^+ ions were consumed by the ionization of NH_2 groups). Furthermore, increasing the polymer concentration enhances both the ionic strength (i.e., a higher number of $-^+N(CH_3)_3$ groups and Cl^- ions) and the number of NH_2 groups, causing an increase in the pH of the solution.

The conductivity of the WSC solutions was measured at 25 °C and compared to the theoretical values that were calculated using eqs 2 and 3. As shown in Figure 5, the theoretical values obtained for conductivity were in good agreement with the values obtained by experimental measurement. Dissolving WSC in deionized water generates charged trimethylated ammonium ($-(CH_3)_3N^+$) and Cl^- ions; thus, an increase in the polymer concentration and DS increases the number of ions in solution (Figure 5a). In a similar manner, an increase in the concentration of NaCl also results in an increase in the conductivity of the solutions due to an increase in the number of ions (Figure 5b).

Rheological Properties of WSC Solutions. The dynamic mechanical properties of a polymeric solution are generally dependent on its concentration.[46−48] In the dilute regime, the

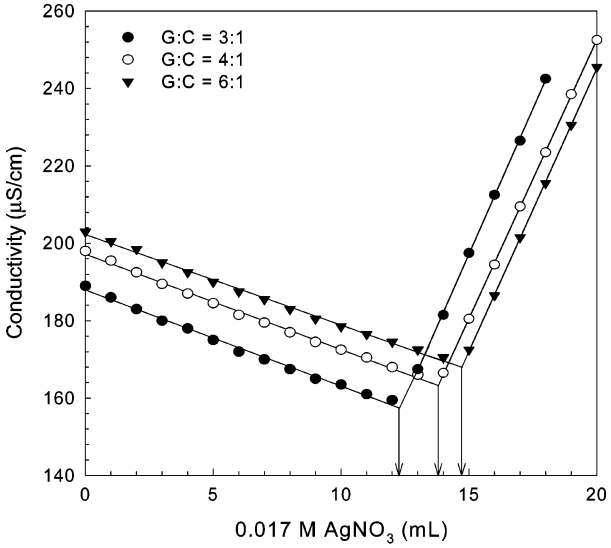

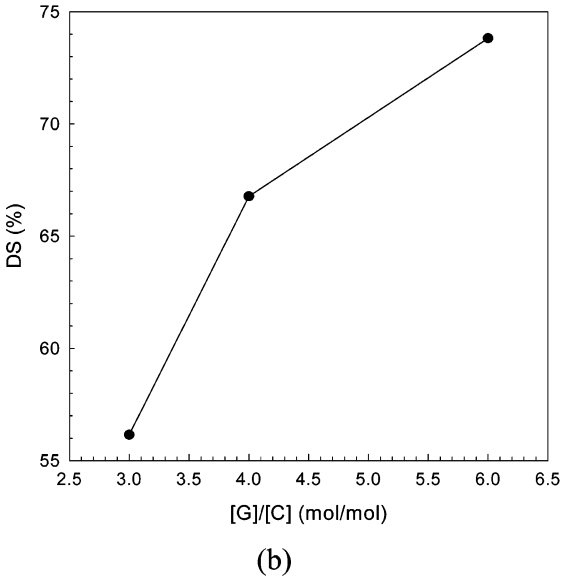

Figure 3. (a) Conductivity of WSCs as a function of volume of $AgNO_3$ added at 25 °C. (b) The percent of DS determined as a function of the molar ratio of GTMAC to chitosan, [G]/[C].

macromolecules are separated from each other in solvent. Thus, the physical properties are mainly controlled by the hydrodynamic volume and the conformation of the polymeric molecules.[40] However, in the concentrated regime, the rheological properties are greatly dependent on the number of intermolecular entanglements between the macromolecules. The boundary between the dilute and concentrated regimes is determined by the critical concentration (C_C), which is the concentration at which the polymer chains start to entangle.

A dilute solution is defined as having a polymer concentration (C) that is less than C_C, while a concentrated solution has a concentration that is greater than C_C.[49] Figure 6 shows the viscosity of all WSC solutions in terms of DS and salt concentration over a broad range of polymer concentrations (i.e., 0 to 10 g/dL). The C_C was determined from the crossover point of the two independent slopes for the dilute and concentrated regimes. The values for C_C were found to gradually decrease as the DS and salt concentration were increased with a value for C_C between 1 and 2 g/dL for all solutions investigated. In the dilute regime, the reduced viscosity (η_{red}) of the WSC with

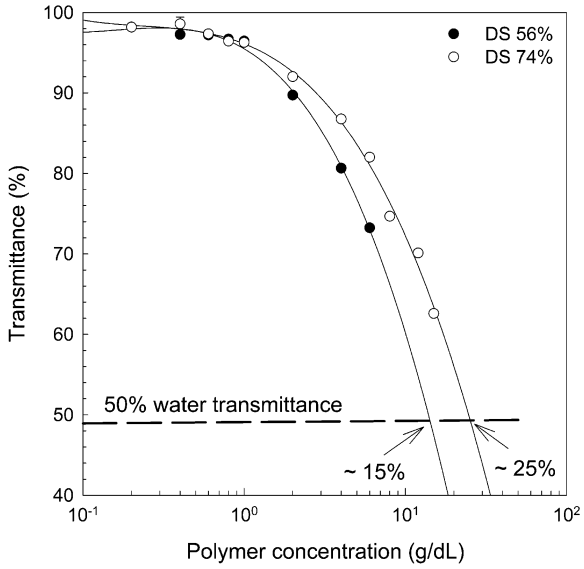

Figure 4. UV−visible absorbance measurements for WSCs with low and high DS. The experimental data were fit using a polynomial function ($R^2 = 0.99$) in order to obtain the theoretical curve. The water solubility of WSCs at room temperature was determined via extrapolation of the fitted curve to 50% of the transmittance measurement obtained for water under these conditions (as described in the Experimental Section under Measurement of Water Solubility of WSCs).

Table 3. Measured pH Values for the WSC Solutions with DS of 56%, 67%, and 74% as a Function of Polymer Concentration and Ionic Strength

	DS = 56% 0 M NaCl	DS = 56% 0.02 M NaCl	DS = 56% 0.1 M NaCl	DS = 67% 0.1 M NaCl	DS = 74% 0.1 M NaCl
C (g/dL)	pH	pH	pH	pH	pH
0.02	6.25	6.79	6.89	6.72	6.47
0.05	6.46	6.84	7.19	6.86	6.61
0.07	6.64	7.07	7.23	6.87	6.74
0.1	6.71	7.22	7.38	7.16	6.77
0.3	7.18	7.32	7.57	7.30	6.97
0.5	7.24	7.62	7.80	7.44	7.24

DS of 56% was found to be highly dependent on the concentration of salt (Figure 6a). In the absence of NaCl, η_{red} increased when the polymer concentration decreased below C_C. This follows the typical rheological behavior for a polyelectrolyte solution at low ionic strength.[50−52] The relationship between the viscosity and concentration of a polyelectrolyte in the dilute regime can be described by the Fuoss equation as follows:[53,54]

$$\eta_{red} = \frac{\eta_{sp}}{C} = \frac{A}{1 + BC^{1/2}} \quad (16)$$

where η_{sp} is the specific viscosity, C is the concentration of electrolyte, and A and B are the empirical constants. From eq 16, the viscosity of the polyelectrolyte solution is inversely proportional to the square root of the polymer concentration ($\eta \sim C^{-1/2}$). In the dilute regime and in the absence of salt, the viscosity of a polyelectrolyte solution is known to increase with a decrease in the polymer concentration. This behavior can be explained by the higher Coulombic repulsions between the charged groups (due to a decrease in the shielding effect) which causes an increase in the volume of the polymer backbone.[50] However, in the presence of salt, the viscosity was found to increase exponentially with an increase in the concentration of WSC (Figure 6a). Below C_C, the power-law relationship was $\eta_{red} \sim C^{0.18\pm0.04}$ (or $\eta_{sp} \sim C^{1.18\pm0.04}1$) when the concentration

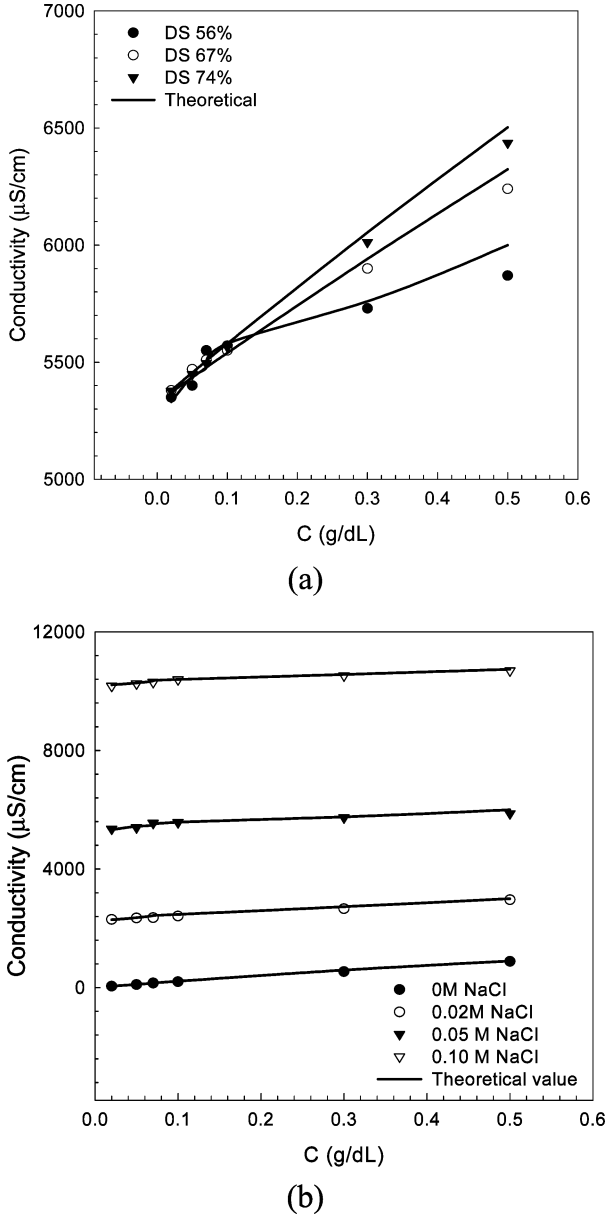

Figure 5. (a) The effect of the DS on the conductivity of WSCs as measured in the presence of 0.05 M NaCl and (b) the effect of NaCl concentration on the conductivity of WSC with a DS of 56%. All measurements were performed at 25 °C. The theoretical conductivity was predicted from eqs 2 and 3.

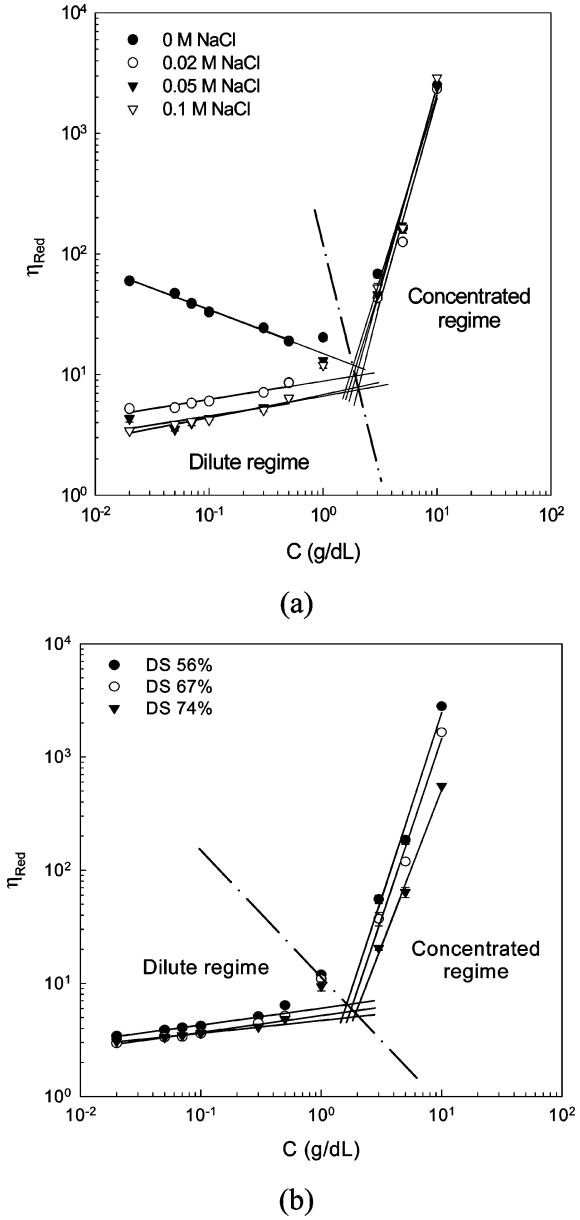

Figure 6. The reduced viscosity (η_{red}) as determined by varying the (a) salt concentration in a 56% DS WSC solution and (b) DS of WSC in the presence of 0.10 M NaCl. All measurements were performed at 25 °C.

of NaCl ranged from 0.02 to 0.1 M. In the concentrated regime ($C > C_C$), the power-law index was 3.26 ± 0.15 for η_{red} vs C and 4.26 ± 0.15 for η_{sp} vs C regardless of the salt concentration (Figure 6a).

The effect of DS on the viscosity of the WSC solution in the presence of 0.1 M NaCl is shown in Figure 6b. The power-law index was 0.15 ± 0.02 (or 1.15 ± 0.15 for η_{sp} vs C) in the dilute regime and 3.07 ± 0.16 (or 4.07 ± 0.16 for η_{sp} vs C) in the concentrated regime regardless of the DS value. The dependence of the viscosity on the polymer concentration has been previously studied in the concentrated regime. For example, Dobrynin et al.[55] theoretically predicted a power-law index value of 3.75 from the relationship between the η_{sp} and the polymer concentration for semidilute entangled solutions of a polyelectrolyte in the presence of excess salt. The power-law index values obtained in our study were slightly higher (i.e., 4.07) than the reported theoretical value of 3.75. The difference between the calculated and theoretical values may be explained by the consideration of two factors. First, as proposed by Amiji,[56] intermolecular hydrophobic interactions ($-CH_3$) increase the contact between the polymer molecules. Second, electrostatic repulsion forces exerted by the quaternary ammonium ions may not be completely screened by the salt anions. Thus, the intramolecular electrostatic repulsions may result in an increase in the molecular size (or volume) of the individual polymer molecules, which eventually leads to an increase in the degree of physical contact between the macromolecules. The formation of these physical contacts may result in a higher power-law index value (~4.0). Hwang et al.[57] measured the viscosity as a function of chitosan concentration in 0.1 M AcOH/0.1 M NaCl at 25 °C. From their results, the viscosity increased exponentially with an increase in the chitosan concentration with a power-law index of 3.94 (i.e., $\eta_{sp} \sim C^{3.94}$). Desbrieres[43] reported an exponent of 5.2 (i.e., $\eta_{sp} \sim C^{5.2}$) for a chitosan solution in 0.3 M AcOH/0.1 M AcONa.

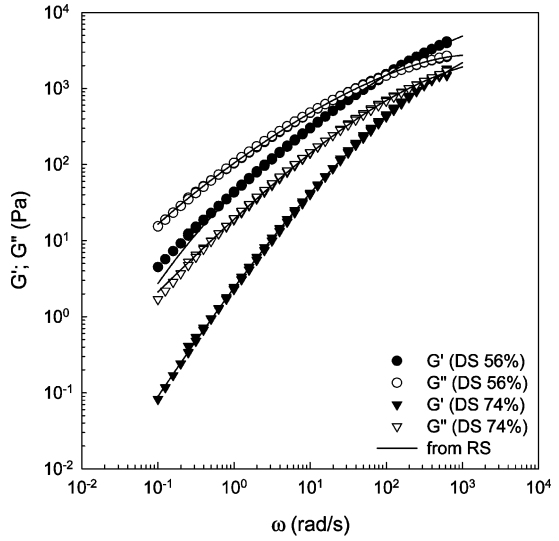

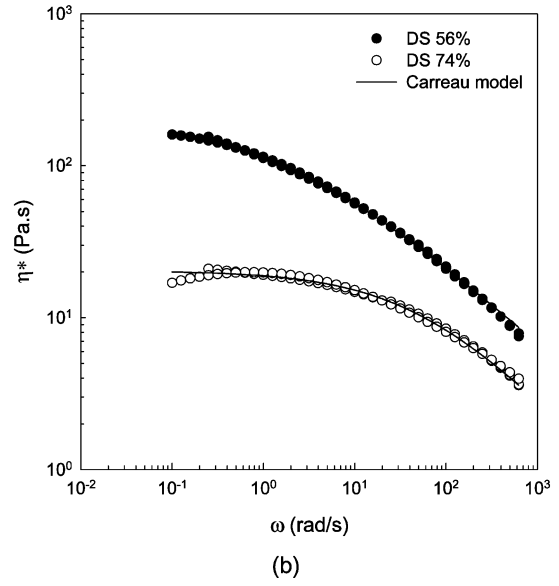

Figure 7. (a) Storage modulus (G'), loss modulus (G''), and (b) complex viscosity (η^*) of the 56% DS and 74% DS WSCs (15 g/dL aqueous solution) as a function of frequency.

Small-amplitude oscillatory shear tests were preformed in the linear viscoelastic zone (LVZ), where the complex moduli G' and G'' are independent of the magnitude of deformation applied. As shown in Figure 7, the rheological properties were dependent on the DS value of the WSC at a concentration of 15 g/dL at 25 °C. At lower DS, an increase in the complex moduli (Figure 7a) and viscosity (Figure 7b) were observed. In the high-frequency zone (HVZ), the viscosity gradually decreased with increasing frequency (ω), corresponding to shear-thinning behavior (Figure 7b). The slope (or shear-thinning power index) in the HVZ increased with an increase in the DS (i.e., 0.45 for 56% DS and 0.57 for 74% DS). This result indicates that the lower DS WSC solutions have a larger number of physical contacts between the macromolecules, which in turn restricts the motion of each macromolecular chain. Therefore, for solutions containing a lower DS WSC, a longer time is required to replace the broken entanglements that occurred from the applied strain. Thus, non-Newtonian (or shear-thinning) behavior is more prevalent for the WSC with lower DS. The variation of the number of physical interactions between the

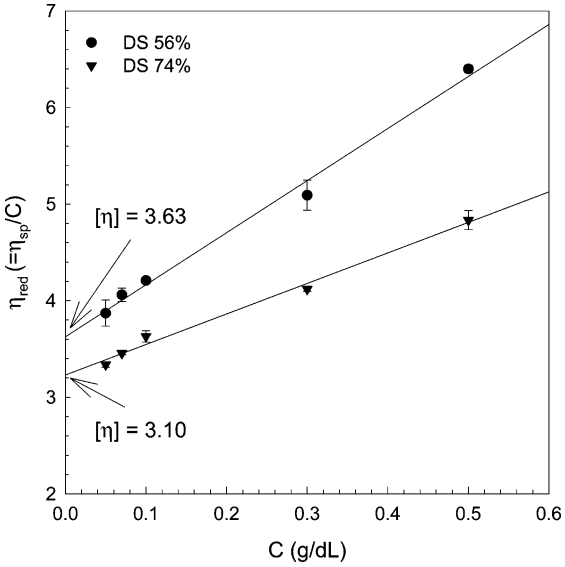

Figure 8. Reduced viscosity (η_{red}) of 56% and 74% DS WSCs measured as a function of WSC concentration in the presence of 0.1 M NaCl. The intrinsic viscosity ([η]) was determined by extrapolating the η_{red} to a WSC concentration of 0 g/dL.

56% and 74% DS WSCs may be explained by the molecular weight of each polymer. The molecular weight of each WSC was determined by measuring the intrinsic viscosity in 0.1 M NaCl at 25 °C. As shown in Figure 8, the intrinsic viscosity [η] was taken to be the x-intercept of the plot of reduced viscosity (η_{red}) versus polymer concentration. From the plot, [η] was found to be 3.63 dL/g and 3.10 dL/g for the WSCs with DS of 56% and 74%, respectively. The difference in intrinsic viscosities can be explained in terms of the electrostatic repulsion forces and molecular weight. The electrostatic repulsion forces can be generated by the positively charged trimethylated ammonium ions on the WSC chain. The repulsion forces expand the molecular volume of a polyelectrolyte as outlined in the following equation:[58]

$$[\eta] = \frac{10}{3}\pi N_A \frac{(R_h + R_B)^3}{M_P} \quad (17)$$

where N_A represents Avogadro's number, M_P is the molecular weight of the polymer, R_h is the radius of gyration of uncharged macromolecules (or at θ-condition), and R_B is the Bjerrum radius, which corresponds to the expansion of the molecular volume by repulsion forces. The molecular weight of a polymer can be determined from intrinsic viscosity ([η]) using the Mark−Houwink−Sakurada (MHS) equation as follows:[59]

$$[\eta] = KM^{\alpha} \quad (18)$$

where M is the molecular weight and K and α are empirical constants that vary depending on the types of polymer, solvent, and temperature. The electrostatic repulsion forces control the molecular conformation of polyelectrolytes.[60] The molecular conformation can be obtained from the MHS constant α (i.e., $\alpha = 0.5$ for sphere, 0.5−0.8 for random coil, and 1.8 for rod shape).[61] For high electrostatic repulsion forces, the α value increases for linear polyelectrolytes as demonstrated previously for sodium poly(styrene-*p*-sulfonate) (NaPSS)[62] as well as chitosan.[63] At an ionic strength of 0.1 M, the higher DS WSC has stronger electrostatic repulsion forces than the lower DS WSC. The stronger electrostatic repulsion forces result in a

greater expansion of the molecular volume of the polymer chains and a higher value for α. Thus, it is expected from eqs 17 and 18 that the high DS WSC would have higher [η] values. However, the high DS WSC had lower [η] values than the low DS WSC as shown in Figure 8. Therefore, from eq 17 it may be postulated that the lower [η] may be owed to the reduction in molecular weight (M_P). Further evidence of the lower molecular weight for the WSC containing higher DS is provided from consideration of the entanglement concentrations as shown in Figure 6b. The entanglement concentration was 1.45 g/dL for the 56% DS WSC and 1.60 g/dL for the 74% DS WSC. From the literature, lower molecular weight polymers require a higher concentration to form an entanglement.[64] Thus, from the entanglement concentration and the intrinsic viscosity measurements, the higher DS WSC had a lower molecular weight than the low DS WSC. Studies to evaluate the degradation of the WSC during the reaction procedure are in progress.

In this study, the exact K and α values were not known for the aqueous solutions of the WSCs. Thus, rheological parameters were employed to determine the molecular weight distribution (MWD) based on theoretical calculations.[65,66] Thimm et al.[65] demonstrated the relationship between the relaxation time spectrum ($H(\tau)$) and the MWD of polystyrene. Wood-Adams et al.[66] also reported a correlation between the MWD and $H(\tau)$ for polyethylene. In this study, the rheological properties were converted into the stress relaxation spectrum in order to determine the molecular weights of the WSCs. The complex moduli G' and G'' measured in LVZ were employed to calculate the stress relaxation spectrum ($H(\tau)$) from the following equation:[67]

$$G^*(\omega) = \sqrt{G'(\omega)^2 + G(\omega)^2} = \int_{-\infty}^{\infty} (\omega\tau + i)H(\tau)\frac{\omega\tau}{1 + (\omega\tau)^2}\,\mathrm{d}(\ln\tau) \quad (19)$$

where ω is the frequency and τ is the relaxation time. The conversion of the complex moduli G' and G'' to the $H(\tau)$ was performed using the NLREG software package.[68] To verify the calculated relaxation spectra in our study, two standards were employed. First, the G' and G'' values, measured by small oscillatory shear tests, were compared to the theoretical values that were calculated from the relaxation spectra. Second, the zero shear viscosity (η_0) determined from the Carreau model in eq 5 was compared to the area of the relaxation spectra using the following equation:[69]

$$\eta_0 = \lim_{\omega \to 0} \frac{G^*}{\omega} = \int_{-\infty}^{+\infty} \tau H(\tau)\,\mathrm{d}\ln(\tau) \quad (20)$$

Figure 7a shows the complex moduli G' and G'' obtained from the small oscillatory shear tests (circles) and the theoretical values calculated from the stress relaxation spectra (solid lines). A good agreement between the experimentally determined and theoretical values was obtained with the exception of the storage modulus in the low-frequency zone for the 56% DS WSC. In the low-frequency zone, the storage modulus for the 56% DS WSC was found to be solidlike (i.e., $G' = \omega^{0.99}$ and $G'' \sim \omega^{0.83}$). However, in the same frequency zone, the 74% DS WSC displayed a more liquidlike behavior ($G' = \omega^{1.82}$ and $G'' \sim \omega^{1.06}$). The difference between the experimental and calculated values may be expected since the equation for the relaxation time does not account for solidlike behavior. The η_0 values for the 56% DS WSC were 202 Pa.s from the Carreau model and 192 Pa.s from the relaxation spectrum. For the 74% DS WSC, the η_0 values were 20 Pa.s from the Carreau model and 22 Pa.s from the area of the relaxation spectrum. Therefore, the two standards confirm the values obtained for the calculated relaxation spectra.

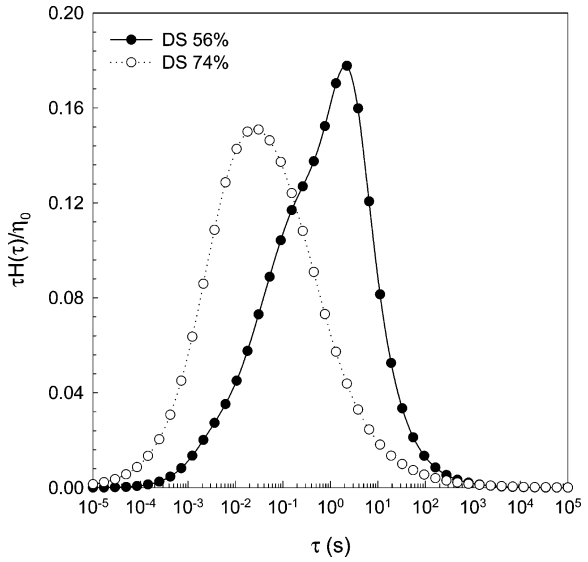

Figure 9. Relaxation curves of WSCs (56% and 74% DS) predicted from eq 18 and the experimental data shown in Figure 6a.

The effect of DS on the normalized stress relaxation spectra (in order to compare the spectra on the same scale[70]) is shown in Figure 9. For the 56% DS WSC, the spectra included a small shoulder at approximately 0.2 s, but the overall shape was monomodal. The 74% DS WSC showed a symmetrical monomodal curve which indicated that the main relaxation mode is independent of the DS value of the WSC. The relaxation time (τ) showed a power relationship with the molecular weight (M) of the polymer: $\tau \sim M^{\Delta}$. The exponent Δ was between 3 and 3.4 depending on the molecular weight of the polymer.[71] Wood-Adams et al.[69] explained that an increase in the molecular weight of the polymer results in an increase in the area under the curve of $\tau H(\tau)$ d lnτ, corresponding to the zero shear viscosity, and shifts the entire curve to longer relaxation times. In our study, the mean relaxation time, τ_m, which corresponds to the relaxation time at the peak in the spectra (i.e., 1.6×10^{-3} to 10 s), was greatly dependent on the DS value of the WSC with a τ_m of 1.9 s for 56% DS and a τ_m of 0.02 s for 74% DS. The 56% DS WSC had a larger area under the spectra or a higher zero shear viscosity (192 Pa.s) than the 74% DS WSC (~22 Pa.s). The longer relaxation time for the 56% DS WSC may be attributed to the higher molecular weight of the polymer, which supports the results obtained from the measurements of the intrinsic viscosity and the entanglement concentration. The high molecular weight of the 56% DS WSC resulted in enhanced dynamic mechanical properties such as G', G'', and η_0, as well as a stronger shear-thinning behavior for this material when compared to the 74% DS WSC. In addition, the rheological properties of the WSCs are dependent on the intensity of various inter- and intramolecular physical interactions. The positively charged dissociated ammonium ions hinder hydrophobic interactions between the $-CH_3$ groups of the WSC macromolecules and also inhibit the formation of hydrogen bonding between the molecular chains via the $-OH$ and $-NH_2$ groups. The WSC with the lower-percentage DS had a reduced degree of molecular electrostatic repulsions, which in turn resulted in a better environment for physical interactions and hence improved the mechanical properties of the polymer solution.

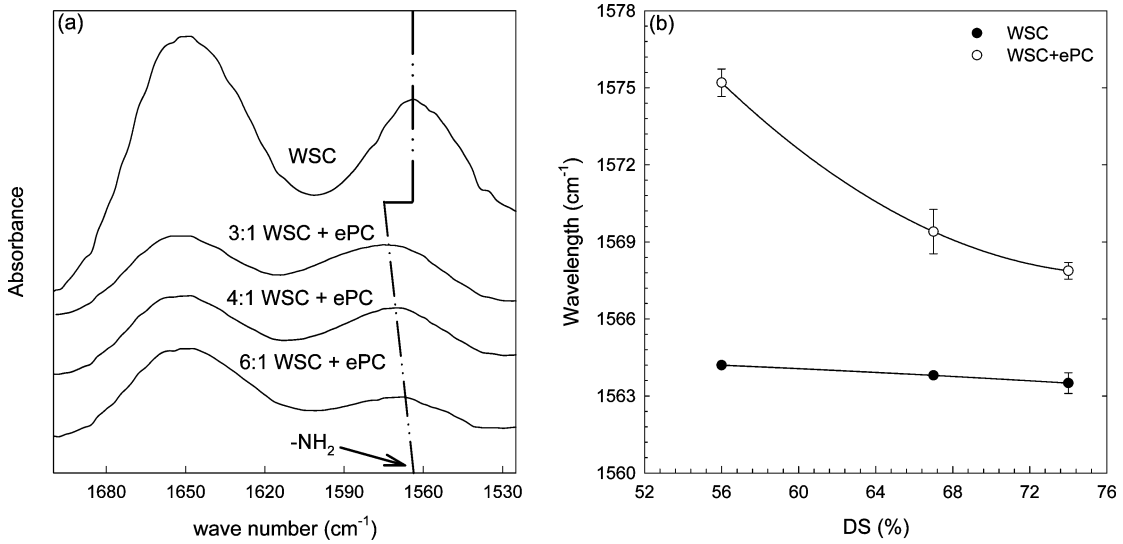

Figure 10. (a) FTIR spectra of WSC and WSC-ePC films and (b) the shift in the $-NH_2$ peak of WSC and WSC-ePC films as a function of the DS of the WSC.

FTIR Analysis of WSC−ePC Films. In a previous report, FTIR analysis was used to demonstrate that the N−H groups on chitosan interact with the lipid ePC.[19] To evaluate the effect of the functionality and DS of the WSC on the potential for interaction with other molecules, films were prepared by blending the WSCs with ePC. The FTIR spectra for WSC (DS ranging from 56% to 74%) and WSC−ePC films are shown in Figure 10a. The average peak position of the NH_2 groups in WSC, varying in DS, was approximately 1564 cm^{-1}. However, when WSC was mixed with ePC, a significant shift in the NH_2 peak was observed. Specifically, the 56% DS WSC had the greatest peak shift for the NH_2 groups from 1564 to 1575 cm^{-1}. The 67% DS WSC NH_2 peak shifted from 1564 to 1569.4 cm^{-1}, and the smallest shift was found for the 74% DS WSC to 1567.9 cm^{-1} (Figure 10b). Therefore, the 56% DS WSC had the greatest degree of interaction with ePC, indicating that a lower DS WSC may be more suitable for preparing stable film or gel systems.

Conclusion

A water-soluble chitosan derivative (WSC) that was soluble in water up to concentrations of 25 g/dL was prepared by conjugating GTMAC onto chitosan chains. The higher water solubility and cationic nature of WSC makes this polymer an attractive biomaterial for pharmaceutical use. The positively charged WSC may be complexed with negatively charged peptides (e.g., insulin) or DNA for development of pharmaceutical formulations or delivery systems for these molecules. In addition, its solubility at physiological pH may enhance its potential use for fabrication of biomedical devices. From the WSC−ePC films prepared, the lower DS WSC had the strongest interaction with the lipid ePC. The combination of WSC and ePC could be used to prepare composite films for use as implantable localized drug delivery systems. Future studies in our laboratory will focus on evaluating the biocompatibility of WSC−ePC films and characterizing the use of WSC as a biomaterial for implant systems.

Acknowledgment. The authors gratefully acknowledge the financial support of Natural Sciences and Engineering Research Council of Canada (NSERC) and Ontario Cancer Research Network (OCRN).

References and Notes

(1) Singla, A. K.; Chawla, M. *J. Pharm. Pharmacol.* **2001**, *53*, 1047−1067.
(2) Roberts, G. A. F. *Chitin Chemistry*; MacMillan: London, 1992.
(3) Brugnerotto, J.; Desbrieres, J.; Heux, L.; Mazeau, K.; Rinaudo, M. *Macromol. Symp.* **2001**, *168*, 1−20.
(4) Young, R. J.; Lovell, P. *Introduction to Polymers*, 2nd ed.; Chapman and Hall: London, 1991.
(5) Kim, S. K.; Rajapakse, N. *Carbohydr. Polym.* **2005**, *62*, 357−368.
(6) Grant, J.; Allen, C. In *Polysaccharides in Drug Delivery and Pharmaceutical Application*; Ravenelle, F., Ed.; American Chemical Society Symposium Series 934; American Chemical Society: Washington, DC, 2006; pp 201−225.
(7) Arai, K.; Kinumaki, T.; Fujita, T. *Bull. Tokai Reg. Fish. Res. Lab.* **1968**, *56*, 89−94.
(8) Sanford, P. A. Chitosan: Commercial uses and potential applications. In *Chitin and Chitosan*; Elsevier Applied Science: London, 1989.
(9) Sandford, P. A.; Hutchings, G. P. Chitosan − A natural, cationic biopolymer: Commerical applications. In *Industrial Polysaccharides: Genetic Engineering, Structure/Property Relations and Applications*; Elsevier Science Publishers: Amsterdam, 1987.
(10) Jayakumar, R.; Prabaharan, M.; Reis, R. L.; Mano, J. F. *Carbohydr. Polym.* **2005**, *62*, 142−158.
(11) Kumar, M. N. V. R. *React. Funct. Polym.* **2000**, *46*, 1−27.
(12) Jackson, D. S. Johnson & Johnson Products, Inc., U.S.A., 1987.
(13) Chenite, A.; Buschmann, M.; Wang, D.; Chaput, C.; Kandani, N. *Carbohydr. Polym.* **2001**, *46*, 39−47.
(14) Allan, G. G.; Altman, L. C.; Bensinger, R. E.; Ghosh, D. K.; Hirabayashi, Y.; Neogi, A. N.; Neogi, S. Biomedical applications of chitin and chitosan. In *Chitin, Chitosan and Related Enzymes*; Academic Press: New York, 1984.
(15) Qin, C. Q.; Du, Y. M.; Xiao, L.; Li, Z.; Gao, X. H. *Int. J. Biol. Macromol.* **2002**, *31*, 111−117.
(16) Maeda, Y.; Kimura, Y. *J. Nutr.* **2004**, *134*, 945−950.
(17) Domard, A. *Int. J. Biol. Macromol.* **1987**, *9*, 98−104.
(18) Khan, T. A.; Peh, K. K.; Ch'ng, H. S. *J. Pharm. Pharm. Sci.* **2000**, *3*, 303−311.
(19) Grant, J.; Blicker, M.; Piquette-Miller, M.; Allen, C. *J. Pharm. Sci.* **2005**, *94*, 1512−1527.
(20) Jumaa, M.; Furkert, F. H.; Muller, B. W. *Eur. J. Pharm. Biopharm.* **2002**, *53*, 115−123.
(21) Connors, K. A.; Amidon, G. L.; Kennon, L. *Chemical stability of pharmaceuticals: a handbook for pharmacists*; Wiley: New York, 1979.
(22) Sashiwa, H.; Kawasaki, N.; Nakayama, A.; Muraki, E.; Yajima, H.; Yamamori, N.; Ichinose, Y.; Sunamoto, J.; Aiba, S. *Carbohydr. Res.* **2003**, *338*, 557−561.

(23) Chen, W. R.; Liu, H.; Ritchey, J. W.; Bartels, K. E.; Lucroy, M. D.; Nordquist, R. E. *Cancer Res.* **2002**, *62*, 4295−4299.
(24) Xu, F.; Liu, H.; Wu, X. Z.; Jiang, H. Y.; Nordquist, R. E.; Chen, W. R. *Med. Phys.* **1999**, *26*, 1371−1374.
(25) Kean, T.; Roth, S.; Thanou, M. *J. Controlled Release* **2005**, *103*, 643−653.
(26) Sieval, A. B.; Thanou, M.; Kotze, A. F.; Verhoef, J. E.; Brussee, J.; Junginger, H. E. *Carbohydr. Polym.* **1998**, *36*, 157−165.
(27) Thanou, M.; Florea, B. I.; Geldof, M.; Junginger, H. E.; Borchard, G. *Biomaterials* **2002**, *23*, 153−159.
(28) Seong, H. S.; Whang, H. S.; Ko, S. W. *J. Appl. Polym. Sci.* **2000**, *76*, 2009−2015.
(29) Nam, C. W.; Kim, Y. H.; Ko, S. W. *J. Appl. Polym. Sci.* **2001**, *82*, 1620−1629.
(30) Qin, C. Q.; Xiao, Q.; Li, H. R.; Fang, M.; Liu, Y.; Chen, X. Y.; Li, Q. *Int. J. Biol. Macromol.* **2004**, *34*, 121−126.
(31) Remyheintz, N.; Bali, J. P.; Senelar, R.; Gastaud, J. M. *C. R. Acad. Sci., Ser. III:* **1993**, *316*, 1363−1367.
(32) Gastaud, J. M.; Senelar, R.; Pujol, H. *C. R. Acad. Sci., Ser. III:* **1998**, *321*, 5−10.
(33) Miya, M.; Iwamoto, R.; Yoshikawa, S.; Mima, S. *Int. J. Biol. Macromol.* **1980**, *2*, 323−324.
(34) Kasaai, M. R.; Arul, J.; Charlet, C. *J. Polym. Sci., Part B: Polym. Phys.* **2000**, *38*, 2591−2598.
(35) Lim, S. H.; Hudson, S. M. *Carbohydr. Res.* **2004**, *339*, 313−319.
(36) Park, J. H.; Cho, Y. W.; Chung, H.; Kwon, I. C.; Jeong, S. Y. *Biomacromolecules* **2003**, *4*, 1087−1091.
(37) Savarmand, S.; Carreau, P. J.; Bertrand, F.; Vidal, D. J. E.; Moan, M. *J. Rheol.* **2003**, *47*, 1133−1149.
(38) Lide, D. R. *CRC Handbook of Chemistry and Physics*, 85th ed.; CRC Press: Boca Raton, FL, 2004.
(39) Coury, L. *Curr. Sep.* **1999**, *18*, 91−96.
(40) Macosko, C. W. *Rheology: principles, measurements, and applications*; VCH: New York, 1994.
(41) Cox, W. P.; Merz, E. H. *J. Polym. Sci.* **1958**, *28*, 619−622.
(42) Carreau, P. J.; De Kee, D.; Chhabra, R. P. *Rheology of polymeric systems: principles and applications;* Hanser/Gardner Publications: Munich, 1997.
(43) Desbrieres, J. *Biomacromolecules* **2002**, *3*, 342−349.
(44) Alberty, R. A.; Silbey, R. J. *Physical Chemistry*, 2nd ed.; Wiley: New York, 1997.
(45) Morel, F. O.; Hering, J. G. *Principles and Applications of Aquatic Chemistry*; Wiley: New York, 1993.
(46) Colby, R. H.; Fetters, L. J.; Funk, W. G.; Graessley, W. W. *Macromolecules* **1991**, *24*, 3873−3882.
(47) Heo, Y.; Larson, R. G. *J. Rheol.* **2005**, *49*, 1117−1128.
(48) Yang, H. Y.; Yan, Y. F.; Zhu, P. P.; Li, H.; Zhu, Q. R.; Fan, C. G. *Eur. Polym. J.* **2005**, *41*, 329−340.
(49) Kulicke, W.-M.; Clasen, C. *Viscosimetry of polymers and polyelectrolytes*; Springer: Berlin, 2004.
(50) Kienzlesterzer, C.; Rodriguezsanchez, D.; Rha, C. *J. Appl. Polym. Sci.* **1982**, *27*, 4467−4470.
(51) Antonietti, M.; Briel, A.; Forster, S. *J. Chem. Phys.* **1996**, *105*, 7795−7807.
(52) Liaw, D. J.; Huang, C. C. *J. Appl. Polym. Sci.* **1997**, *63*, 175−185.
(53) Fuoss, R. M. *J. Polym. Sci.* **1948**, *3*, 603−604.
(54) Fuoss, R. M. *J. Polym. Sci.* **1949**, *4*, 96−96.
(55) Dobrynin, A. V.; Colby, R. H.; Rubinstein, M. *Macromolecules* **1995**, *28*, 1859−1871.
(56) Amiji, M. M. *Carbohydr. Polym.* **1995**, *26*, 211−213.
(57) Hwang, J. K.; Shin, H. H. *Korea-Aust. Rheol. J.* **2000**, *12*, 175−179.
(58) Antonietti, M.; Briel, A.; Forster, S. *Macromolecules* **1997**, *30*, 2700−2704.
(59) Painter, P. C.; Coleman, M. M. *Fundamentals of Polymer Science: an Introductory Text*, 2nd ed.; Technomic Publishing Co.: Lancaster, PA, 1997.
(60) Miyamoto, S.; Ishii, Y.; Ohnuma, H. *Macromol. Chem. Phys.* **1981**, *182*, 483−500.
(61) Chen, R. H.; Tsaih, M. L. *Int. J. Biol. Macromol.* **1990**, *23*, 135−141.
(62) Takahashi, A.; Kato, T.; Nagasawa, M. *J. Phys. Chem.* **1967**, *71*, 2001−2002.
(63) Tsaih, M. L.; Chen, R. H. *J. Appl. Polym. Sci.* **1999**, *71*, 1905−1913.
(64) Stepanek, P.; Brown, W. *Macromolecules* **1998**, *31*, 1889−1897.
(65) Thimm, W.; Friedrich, C.; Marth, M.; Honerkamp, J. *J. Rheol.* **1999**, *43*, 1663−1672.
(66) Wood-Adams, P. M.; Dealy, J. M. *J. Rheol.* **1996**, *40*, 761−778.
(67) Roths, T.; Maier, D.; Friedrich, C.; Marth, M.; Honerkamp, J. *Rheol. Acta* **2000**, *39*, 163−173.
(68) Honerkamp, J.; Weese, J. *Rheol. Acta* **1993**, *32*, 65−73.
(69) Wood-Adams, P. M.; Dealy, J. M.; Costeux, S. *Abstr. Pap. Am. Chem. Soc.* **2001**, *221*, U396−U396.
(70) Cho, J.; Heuzey, M. C.; Begin, A.; Carreau, P. J. *J. Food Eng.* **2006**, *74*, 500−515.
(71) Vega, J. F.; Rastogi, S.; Peters, G. W. M.; Meijer, H. E. H. *J. Rheol.* **2004**, *48*, 663−678.

BM060436S